The Journal of The Textile Institute

ISSN: 0040-5000 (Print) 1754-2340 (Online) Journal homepage: www.tandfonline.com/journals/tjti20

Fiber-on-fiber friction measurement using hanging fiber method

Azam Alirezazadeh, Mohammad Zarrebini, Mohammad Ghane & Parham Soltani

To cite this article: Azam Alirezazadeh, Mohammad Zarrebini, Mohammad Ghane & Parham Soltani (2018) Fiber-on-fiber friction measurement using hanging fiber method, The Journal of The Textile Institute, 109:5, 636-646, DOI: 10.1080/00405000.2017.1362746

To link to this article: https://doi.org/10.1080/00405000.2017.1362746

Published online: 17 Aug 2017.

Submit your article to this journal

Article views: 396

View related articles

View Crossmark data

Citing articles: 10 View citing articles

Slick Slide 2003

Full Terms & Conditions of access and use can be found at
https://www.tandfonline.com/action/journalInformation?journalCode=tjti20

THE JOURNAL OF THE TEXTILE INSTITUTE, 2018
VOL. 109, NO. 5, 636–646
https://doi.org/10.1080/00405000.2017.1362746

Taylor & Francis
Taylor & Francis Group

Check for updates

Fiber-on-fiber friction measurement using hanging fiber method

Azam Alirezazadeh, Mohammad Zarrebini, Mohammad Ghane and Parham Soltani

Department of Textile Engineering, Isfahan University of Technology, Isfahan, Iran

ABSTRACT

Estimation and evaluation of frictional behavior of delicate materials such as textile fibers is contingent upon existence of accurate experimental methods. In this work, the effect of fiber fineness on frictional behavior of polypropylene fibers was investigated using a developed high-precision experimental setup based on hanging fiber method. Fiber fineness was varied by varying the spinning pump speed during production of melt-spun fibers on an industrial scale melt spinning machine. Data acquisition was achieved using Delphi programming software. A geometrical model capable of evaluating the frictional force between two in-contact identical fibers was proposed. Fiber-on-fiber frictional force was expressed by a third degree polynomial function of fiber diameter. The least value of frictional force was found to belong to fiber diameter of 49.1 μm which corresponds to linear density of 15.5 den. It was concluded that frictional behavior of fibers is influenced by factors such as contact point geometry, rate of fiber strain and profile of generated heat.

ARTICLE HISTORY
Received 15 April 2017
Accepted 26 July 2017

KEYWORDS
Friction; hanging fiber method; frictional force; polypropylene; fiber fineness

1. Introduction

Friction is an important property of textile materials that affects their desirable processing and performance. Friction is important in cases such as needle punching process, carding and spinning of yarns, wool felting, abrasion, and wear of cloth (P. Soltani & M. S. Johari, 2012). Despite conduction of vast amount of researches on various aspects of frictional behavior of textiles, the subject still is one of the most complicated, partly understood, and difficult to control phenomenon associated with textiles. Friction phenomenon arises from interaction between two in-contact surfaces. Factors affecting this interaction system either individually or collectively are bound to influence the frictional behavior of the two surfaces. Numerous investigations with the aim of measuring or understanding this phenomenon have been conducted. These investigations have led to classification of the relevant factors into material-related and process-related categorizes. While the former includes fiber morphology factors such as surface features, cross-sectional shape, dimensions, surface lubricant, and molecular orientation, the latter includes normal force between the two surfaces, contact area, sliding speed, and the environmental conditions (Marcicano, Tu, & Rylander, 2004; Rajanala, 2007; Wang et al., 2016).

Measurement of polymers friction coefficient is rather difficult due to mobility of polymer chains as the result of the contact stress, speed, temperature and lack of validated experimental method. Gustafsson (2013) experimentally evaluated the static and dynamic friction coefficients of polyoxymethylene and polyamides, using interaction system between a steel sphere and polymeric surface. Rusu, Daniela, Benchea, Carlescu, and Olaru (2016) and Rusu, Ionita, Cârlescu, Prisacaru, and Olaru (2015) experimentally determined the frictional resistance and friction coefficient between a steel cylinder and polyurethane surface. Cho, Bhushan, and Dyess (2016) explored the effects of speed, pressure and dwell time on the static and dynamic friction of polypropylene, polyester, and high-density polyethylene pair surfaces. While the effect of speed and pressure was elucidated in terms of changes in roughness and wear of surface, the effect of dwell time was explained in terms of macro/nano-creep.

Generally, the classical laws of friction are not applicable to textile materials in the sense that is used for metallic materials. For this reason, various modified theories suitable to friction in textile materials have been developed (Briscoe, 1996; Briscoe & Kremnitzer, 1979; Briscoe & Tabor, 1978; Cornelissen, de Rooij, Rietman, & Akkerman, 2014; Gao, Wang, & Hao, 2015; Rajanala, 2007; Ramkumar, 1998). According to Ramkumar (1998) the major factor which affects the frictional force between two polymeric surfaces is the area of contact. This depends on the surface geometry, roughness, contact time, and the exerted load on the contact area. In addition to the contact area, sliding of two surfaces relative to each other also depends on plowing or shearing of in-contact surfaces. According to the work of Ramkumar, Equation (1) gives the total frictional resistance (F):

$$F = A \times S + P \tag{1}$$

where A, S and P denote apparent contact area, shear strength and plowing component, respectively.

Briscoe and Kremnitzer (1979) believe that $A \times S$ and P as two parameters independently contribute to the net frictional

CONTACT Parham Soltani pa.soltani@cc.iut.ac.ir

© 2017 The Textile Institute

force. In a related study, Briscoe and Tabor (1978) correlated the physical properties to the frictional characteristics of the polymers and concluded that plowing component dominates the frictional losses.

Gralén and Olofsson (1947) studied the frictional force between two fibers twisted at a small angle. It was found that in case of textile fibers, the coefficient of friction changes nonlinearly with the increase in normal load and hence Amontons' law cannot be applied to fibers. According to the work of Gralen, Equation (2) gives the frictional force:

$$F = aW + bW^n \tag{2}$$

where F and W denote the frictional force and applied normal load, n is the number of twist turns, and a and b are the frictional parameters which are determined by empirical curve fitting.

In the same year, Makinson (1952) proposed Equation (3) for calculating the frictional force:

$$F = b + aW^n \tag{3}$$

Equation (3) parametrically is the same as Equation (2).

Ajayi (1992) characterized the frictional behavior of fibers in terms of parameters such as frictional resistance, force amplitude and static and dynamic frictional forces. The influence of variables such as normal force, sliding velocity, sliding frequency, and the nature of surfaces on coefficient of friction was investigated. It was observed that the coefficient of friction decreases with an increase in normal force. It was also concluded that the frictional force and normal force are not linearly related and Equation (4) was proposed:

$$F = aW^n \tag{4}$$

where a and n represent empirical constants whose values are found by fitting the data on the model using a least square analysis.

Howell and Mazur (1953) introduced hanging fiber method which is based on point-contact technique for measuring frictional behavior of the fibers. Using this method, Howell (1953) measured friction of a fiber in contact with a cylinder and dependency of friction on cylinder radius was investigated. It was found that cylinders of larger radius are associated with higher values of n in Equation (4), thus higher frictional force. It must be pointed out that this finding is based on using just two diametrically different cylinders and therefore, it cannot be regarded as a general conclusion applicable to all types of fibers.

The conducted research works on frictional behavior of textile fibers are mostly exclusive of synthetic fibers and inclusively treat natural fibers such as wool, mohair, cotton, jute, and long vegetable fibers (Bandyopadhyay, 1951; Basu, Hamza, & Sikorski, 1978; Campos, Bechtold, & Rohrer, 2003; Martin & Mittelmann, 1946; Nair, Sheela, Vivekanandan, Patwardhan, & Nachane, 2013; Oxenham & Hassanin, 1995; Sinoimeri, 2009). These studies have highlighted the effect of surface characteristics and histological structure of natural fibers on frictional properties. Nair et al. (2013) assuming Amontons' law applies, investigated frictional characteristics of cotton fibers and stated that coarser fibers show higher coefficient of friction.

The above review is by no means exhaustive; however, it vividly demonstrates the scarcity of research on the effect of fiber fineness on frictional force, in general, and in particular fiber-on-fiber friction. Fiber-on-fiber friction is one of the most important fiber characteristics both in non-woven manufacturing processes and the performances of the final products (Soltani, Johari, & Zarrebini, 2015). While the integrity of woven or knitted fabrics arises from thread interlacing, the integrity of non-woven fabrics is mostly due to fiber-on-fiber friction. Currently, polyolefin fibers have gained the highest usage in various fields of non-woven industry (Soltani, Zarrebini, Laghaei, & Hassanpour, 2017). Since according to our search of literature, fiber-on-fiber friction of polypropylene fibers has ever been investigated, therefore, this study investigates the effect of fiber fineness on frictional behavior of polypropylene fibers using a developed experimental setup based on hanging fiber method. Additionally, in order to enhance the accuracy of the results, some modifications are proposed for elimination of noises that adversely affect friction trace.

2. Theory of fiber friction in hanging fiber method

Howell and Mazur (1953) proposed the hanging fiber method for measuring the frictional force between two in-contact fibers. In this method, one of the fibers is stretched horizontally over a holder and clamped at both ends. One end of the second fiber is fixed at a point above the holder and the fiber is passed over the first fiber at an angle of 90°, while its free end is attached to a defined weight. During the test, the vertical fiber is kept stationary and the horizontal fiber first moves downward in a distance of d and then returns back to its initial position. Figure 1 shows the force diagram of the system under equilibrium.

Frictional force between two in-contact fibers is obtained using a power law of friction (Equation (5)) for fibrous materials proposed by Howell (1951) and Howell and Mazur (1953)

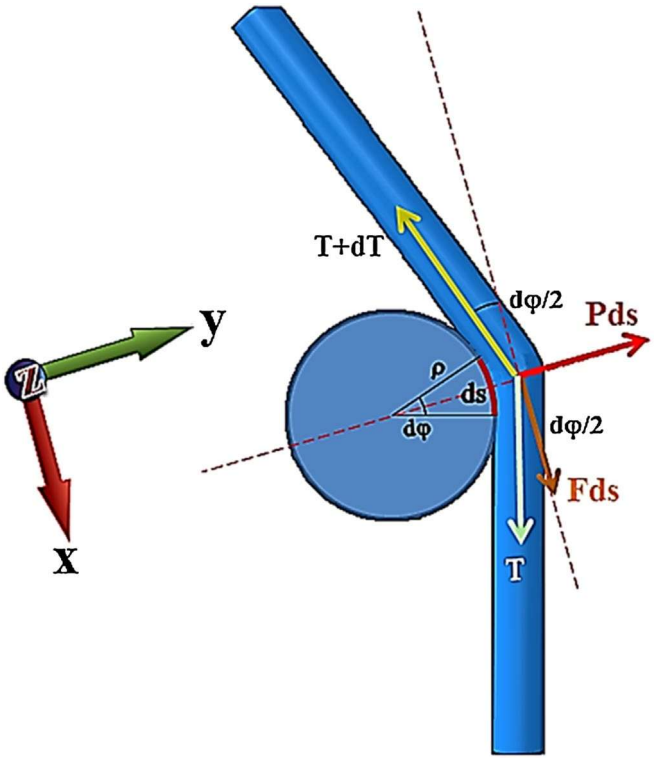

Figure 1. Force equilibrium diagram during friction test.

which is also confirmed by other researchers such as (Abdellahi, Naghashzargar, & Semnani, 2016; Abdellahi, Naghashzargar, & Semnani, Attaway, 1999; Guthrie & Oliver, 1952; King, 1950; Lincoln, 1954). This model seems to be the most widely accepted among all the models proposed for fibrous materials Bhushan, (2013).

$$F = aP^n \tag{5}$$

where F denotes the frictional force, P is the normal load, and a and n are frictional constants. The last two parameters are referred to as the point-contact friction coefficient and point-contact friction index, respectively. The values of these parameters can be found by curve fitting data.

From Figure 1, Equation (6) is deduced:

$$\mathrm{d}s = \rho \mathrm{d}\varphi \tag{6}$$

where ds is an element of the fiber round the cylinder of radius ρ with the deflection angle of $\mathrm{d}\varphi$.

Resolving forces along x-axis in Figure 1 leads to Equation (7):

$$F\mathrm{d}s = (T + \mathrm{d}T)\cos\left(\frac{\mathrm{d}\varphi}{2}\right) - T\cos\left(\frac{\mathrm{d}\varphi}{2}\right) \cong \mathrm{d}T \tag{7}$$

where T and $T + \mathrm{d}T$ are the tensile forces acting at the ends of element $\mathrm{d}s$.

Substituting Equation (6) in Equation (7):

$$F = \frac{\mathrm{d}T}{\rho \mathrm{d}\varphi} \tag{8}$$

Resolving forces along y-axis in Figure 1 leads to Equation (9):

$$P\mathrm{d}s = T\sin\left(\frac{\mathrm{d}\varphi}{2}\right) + (T + \mathrm{d}T)\sin\left(\frac{\mathrm{d}\varphi}{2}\right) = T\mathrm{d}\varphi \tag{9}$$

where P is the reaction per unit length of the fiber.

Substituting Equation (6) in Equation (9):

$$P = \frac{T}{\rho} \tag{10}$$

Substituting in Equation (5):

$$F = a\left(\frac{T}{\rho}\right)^n \tag{11}$$

Tensile force (T) in the vertical fiber is equal to the applied load by the attached weight (mg). Thus, new form of Equation (11) is as of Equation (12):

$$F = a\left(\frac{\mathrm{mg}}{\rho}\right)^n \tag{12}$$

This equation states that for given values of a and n, the frictional forces for different fibers are equal, when the ratio of weight load to the fiber radius is constant.

Equations (13) and (14) represent the relation between work of friction and the frictional force due to downward and upward displacement d of the horizontal fiber:

$$W_1 = (\mathrm{mg} - F)d\ \tan\mathrm{d}\varphi \tag{13}$$

$$W_2 = (\mathrm{mg} + F)d\ \tan\mathrm{d}\varphi \tag{14}$$

The difference between W_1 and W_2 i.e. (ΔW) is the total work of friction, which corresponds to the area within the friction trace (plot of frictional force vs. displacement):

$$\Delta W = 2Fd\tan\mathrm{d}\varphi \tag{15}$$

or:

$$F = \frac{\Delta W}{2d\ \tan\mathrm{d}\varphi} \tag{16}$$

3. Experimental

3.1. Materials

Arak Petrochemical Company supplied the Moplen Z30S Polypropylene granules. Products such as non-woven fabrics, diapers, medical-sanitary applications, and wipes are made using this polymer. The characteristics of the polymer are presented in Table 1.

3.2. Fibers production

Circular melt-spun polypropylene fibers with fineness of 6.9, 12.6, 18.4, and 22.9 den and density of 0.91 g/cm^3 were produced on a six positions one-stage industrial scale compact melt spinning line. The machine produces around 600 kg/h using circular spinnerets each with 18,000 orifices. Polymer melts in an extruder with L/D ratio of 35. Melting of the polymer granules occurs along the extruder heated by 10 resistance-heating units along the extruder length. A temperature profile of 160–210 °C along the 5600 mm length of extruder together with die pressure of 150 bar was maintained. The molten polymer was then fed to spinning pumps. The take-up speed was set 50 m/min. The required fiber fineness was obtained by varying metering pump speed. Fiber fineness was measured according to ASTM D1577-79 using Lenzing Vibroscope (model 400, Austria). For each set of experiments, 30 samples were tested. The results are presented in Tables 2–5.

3.3. Tensile test of fibers

The stress–strain behavior of single fibers was evaluated according to ASTM D3822 at standard conditions of 20 ± 2 °C and

Table 1. Characteristics of Moplen Z30S polypropylene granules.

Property	Value	Unit	Test method
MFI at 230 °C and 2.16 kg Load	25	g/10 min	ASTM D1238
Density	0.91	g/cm^3	ISO 1183
Flexural modulus	1550	MPa	ASTM D790
Tensile strength	35	MPa	ASTM D638
Elongation	13	%	ASTM D638
Molecular weight	150,000	g/mol	–

Table 2. Levene's test of homogeneity of variances for fiber diameter.

Levene statistic	df1	df2	Sig.
0.052	3	116	0.984

Table 3. Descriptive analysis of mean values of fiber diameter.

					95% confidence interval for mean			
	N	Mean	Std. deviation	Std. error	Lower bound	Upper bound	Minimum	Maximum
1	30	32.8000	3.07753	0.56188	31.6508	33.9492	28.24	37.36
2	30	44.6003	2.93044	0.53502	43.5061	45.6946	40.26	48.94
3	30	53.5003	3.03799	0.55466	52.3659	54.6347	49.00	58.00
4	30	59.6003	3.14481	0.57416	58.4260	60.7746	54.94	64.26
Total	120	47.6252	10.56547	0.96449	45.7155	49.5350	28.24	64.26

Table 4. Levene's test of homogeneity of variances of fiber linear density.

Levene statistic	df1	df2	Sig.
0.079	3	116	0.971

Table 5. Descriptive analysis of mean values of fiber linear density.

					95% confidence interval for mean			
	N	Mean	Std. deviation	Std. error	Lower bound	Upper bound	Minimum	Maximum
1	30	6.9003	1.60751	0.29349	6.3001	7.5006	4.62	9.18
2	30	12.6007	1.52985	0.27931	12.0294	13.1719	10.43	14.77
3	30	18.4043	1.57929	0.28834	17.8146	18.9941	16.15	20.65
4	30	22.9007	1.65846	0.30279	22.2814	23.5199	20.47	25.33
Total	120	15.2015	6.25184	0.57071	14.0714	16.3316	4.62	25.33

$65 \pm 2\%$ relative humidity. Fibers were subjected to uniaxial loading on Zwick CRE tensile tester (model 1446, Germany) using 250 mm gage length at strain rate of 60 mm/min. For each set of experiments, 30 samples were tested.

3.4. Frictional force measurement

Frictional properties of fibers were investigated using a developed experimental setup based on hanging fiber method. Zwick universal testing machine was used during investigation of frictional properties of the sample. The setup completely was housed in an enclosure to minimize the effects of environmental variations like air current and other shocks such as banging of doors. The room is located on the ground floor of the building, which is founded on bedrock to minimize the effect of earth vibration. Prior to the test, fibers were conditioned at temperature of $20 \pm 2\,^{\circ}C$ and relative humidity of $65 \pm 2\%$ for 24 h.

As shown in Figure 2, one end of the vertical fiber is clamped in the upper jaw of the Zwick machine and the free end is attached to a defined weight. The attached weight should not be so light, otherwise a loose junction between fibers is formed. Additionally, the weight should not be so heavy, otherwise as shown in Figure 3, lateral displacement of the horizontal fiber occurs. The lateral displacement prevents point-contact between the two fibers, which is the corner stone of hanging fiber method. Empirically it was found that a lateral displacement of 0.3 cm does not jeopardize accuracy of the results.

In order to ensure existence of stable and constant testing conditions, prior to commencement of each test, the selected weight was attached to the free end of the vertical fiber for 15 s. Two screw clamps were used to bring the fibers into contact and position the horizontal fiber tangentially with the vertical fiber at a point 15.6 cm vertically below the Zwick upper jaw. Under these conditions, the deviation of the weighed fiber from vertical axis was 1.365 cm and the angle of fiber with vertical axis (deflection angle $d\varphi$) was approximately 5° (Figure 2). It must be pointed out that, the deflection angle changes when the horizontal fiber moves vertically, as the result of which the geometry of contact point and hence frictional force changes. Variation in frictional force and changes in geometry of contact point can be limited if the deflection angle is small. It was found that for the small deflection angle of 5°, variation of deflection angle is ±0.56° (Abdellahi et al., 2016; Briscoe & Kremnitzer, 1979). Additionally, the measured forces are always taken as average over the whole movement and therefore, this variation is of practically no importance.

Under the above provisions, the lower table moves down a distance of 2 cm at the rate of 5 mm/min, and again moves back to its initial top position at the same rate. Figure 4(a) presents a typical plot of frictional force (F) vs. displacement (d) obtained through the downward and upward displacement of horizontal fiber. The area within the friction trace shows the total work done by the frictional force. Upon measuring the total work of friction, the frictional force can be calculated using Equation (16).

As is observed in Figure 4, in case of one fiber sliding over another one, which is the situation described by hanging fiber method, the pictorial representation of the sliding action shows stick-slip phenomenon, i.e. in point-contact scenario, sustained sliding does not occurs and the sliding in fact is due to a series of small sticks and slips. In these cases in order to measure frictional force, it is customarily to arbitrarily select a limited number of highest sticks in friction trace, which correspond to 6–10 mm sliding zone on the fiber. The criticism associated with the above lies in the fact that friction test is readily influenced by noises generated by external factors such as air current variation and building vibrations (Figure 4(b)). The noises in turn result in modulation of the friction trace, i.e. increasing the sticks (maximum peaks) and decreasing the slips (minimum peaks), thus

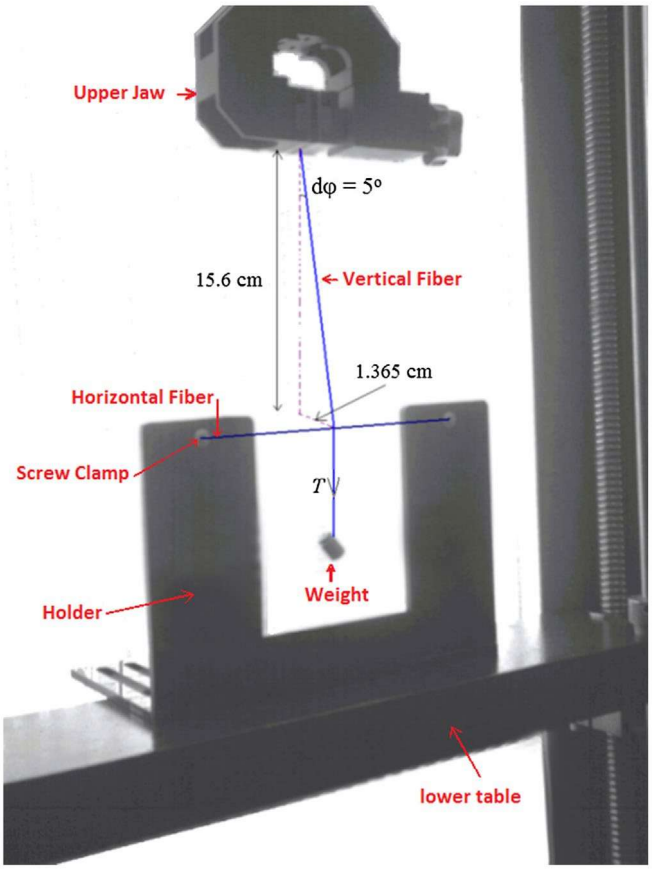

Figure 2. Fiber-on-fiber friction measurement setup.

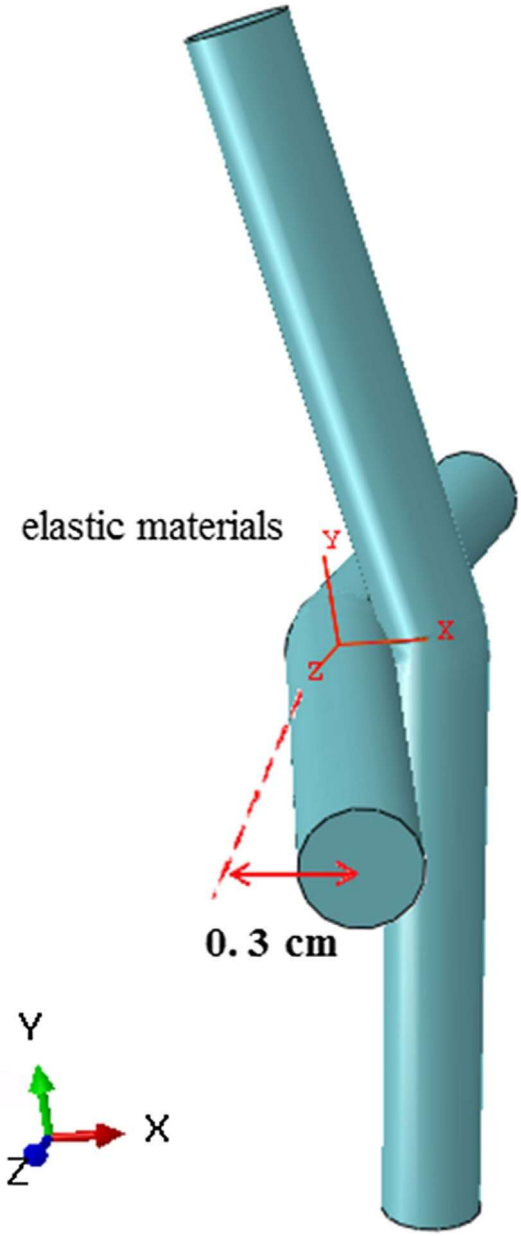

Figure 3. Lateral displacement of horizontal fiber.

introducing errors in the calculated value of frictional force as shown in Figure 5.

As shown in Figure 5, the maximum and minimum peaks in the black trace are elongated due to noise interference and hence the peaks values in the black trace are false. This, in turn, causes error in calculation of work of friction, i.e. the area within the friction trace. As shown in Figure 6(a) environmental noises are symmetrical. Therefore, the superimposing of the noises on friction trace results in equal elongation of the maximum and minimum peaks of the friction trace. Noise elimination can be achieved by replacing each vertical line in friction trace with the middle point of the line (green points) as shown in Figure 6(b). Using this technique, the area formed by connecting the mid points is the true work done by the frictional force. Yellow trace shown in Figure 5 is the filtered version of the trace shown in black. As is observed, noise elimination results in correct selection of the maximum and minimum peaks.

After elimination of noise, work of friction, which corresponds to the area within the friction trace, was calculated using Delphi programming software. Figure 7 shows the operational steps for elimination of symmetrical environmental noises and calculation of work of friction. The procedure involves importing the raw graphs into Delphi software and then elimination of noises from friction trace by replacing each vertical line in friction trace with the middle point of the line. The final step makes an estimate of the area within the friction trace in terms of summation of the pixels within the friction trace and its conversion to the unit of friction work.

4. Results and discussions

Figure 8 shows friction traces for fibers of different fineness. As is observed, the stick-slip phenomenon in case of coarser fibers is more profound in comparison to that of finer fibers. The friction traces for finer fibers are smoother and display much less fluctuation as compared with those of coarser fibers.

In order to calculate frictional force, it is essential to calculate the work of friction. This was achieved by calculation of the area within the friction trace. Frictional force was then calculated using Equation (16). The results of frictional force for different fibers are presented in Table 6. As is observed, frictional force varies with variation of fiber fineness.

The results of friction test were investigated by ANOVA test using SPSS v16.0 software. As shown in Table 7, the significant value is larger than 0.05 indicating that the variances of four data sets are homogenized in confidence interval of 95%. Thus,

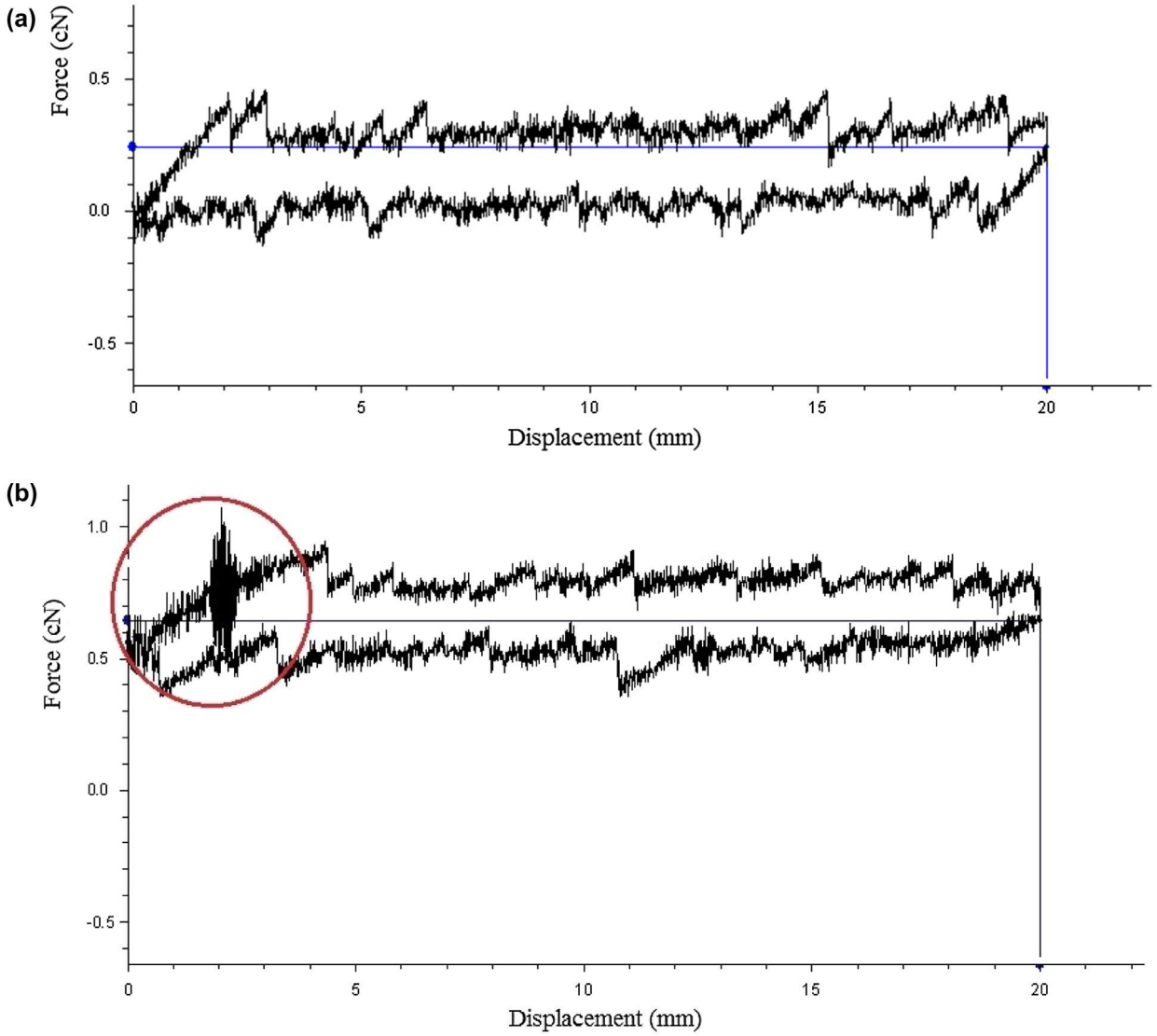

Figure 4. (a) A typical friction trace; and (b) effect of external factor on friction trace.

comparison of the mean values of frictional forces in four data sets is admitted. Descriptive analysis of mean values of frictional forces is shown in Table 8.

Figure 9 shows the relation between mean values of frictional forces and fiber diameter, which is expressed by Equation (17):

$$y = 0.000496x^3 - 0.05467x^2 + 1.7822x - 0.76215 \quad (17)$$

According to Equation (17), the frictional force decreases up to fiber diameter of 49.1 μm which corresponds to linear density of 15.5 den, and then tends to increase with further increases in fiber diameter. The phenomenon observed in this work renders valid due to the followings:

(1) Unlike rigid materials, geometry of contact area in polymeric materials depends upon material hardness (Figure 10) (Dintwa, Tijskens, & Ramon, 2008; Popov & Heß, 2015). The corner stone of the hanging fiber method lies in that fact that the contact area of fibers is a point-contact type, such geometry can be obtained if the fibers are highly stiff (Figure 10(a)). However, polymeric materials such as fibers are deformable and their circular shapes can change at junctions under normal pressure. Therefore, the ideal contact point, such as shown in Figure 10(a), is hard to achieve. The degree of fiber cross-section flattening and change in geometry of contact area depend on fiber diameter (Figure 10(b)) (Zhang, Butz, & Li, 2016).

(2) The Geometry of contact area is also affected by the rate of fiber strain and creep (Kato & Hirasawa, 1996; Rubin et al., 2016). This in turn leads to the changes in stick-slip phenomenon. Figure 11 shows true stress–strain curves for fibers with various diameters, respectively. The following relations are used for converting the engineering stress–strain curve to the true stress–strain curve (P. Soltani & M. Johari, 2012):

$$\text{True strain} = \ln\left(1 + \text{engineering strain}\right)$$

$$\text{True stress} = \text{engineering stress}\,(1 + \text{engineering strain})$$

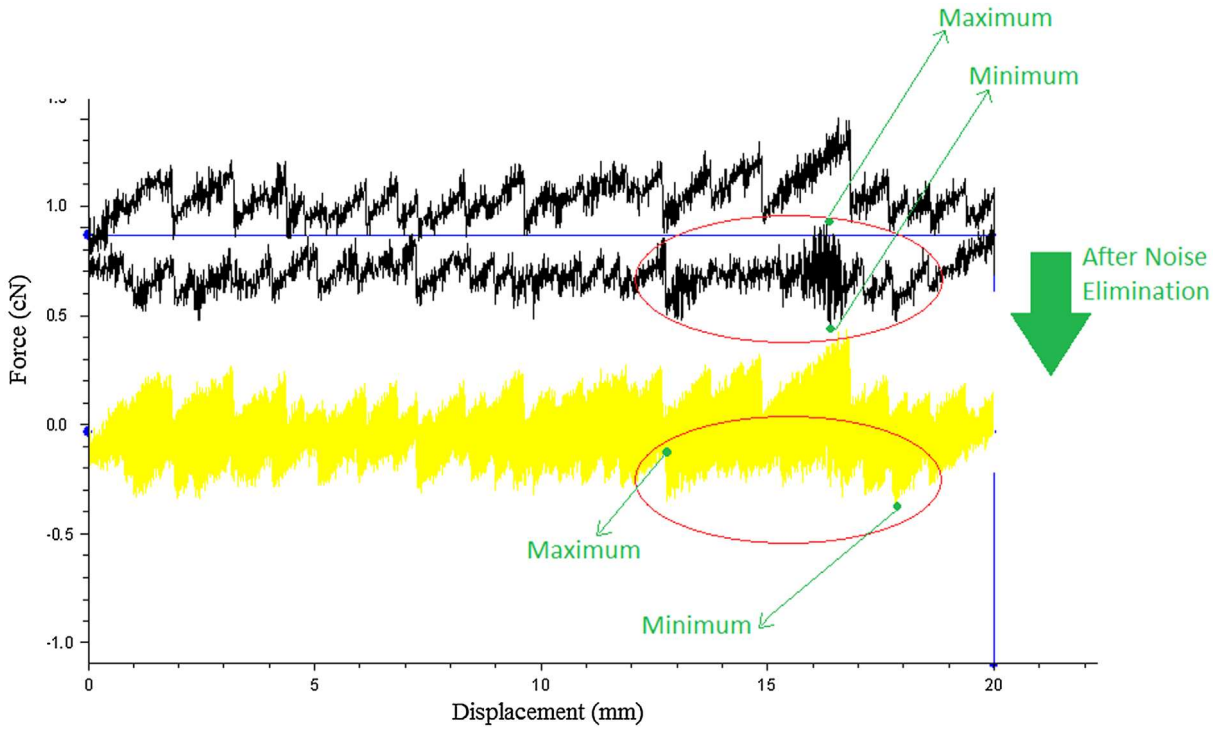

Figure 5. Effect of noise elimination on the friction trace.

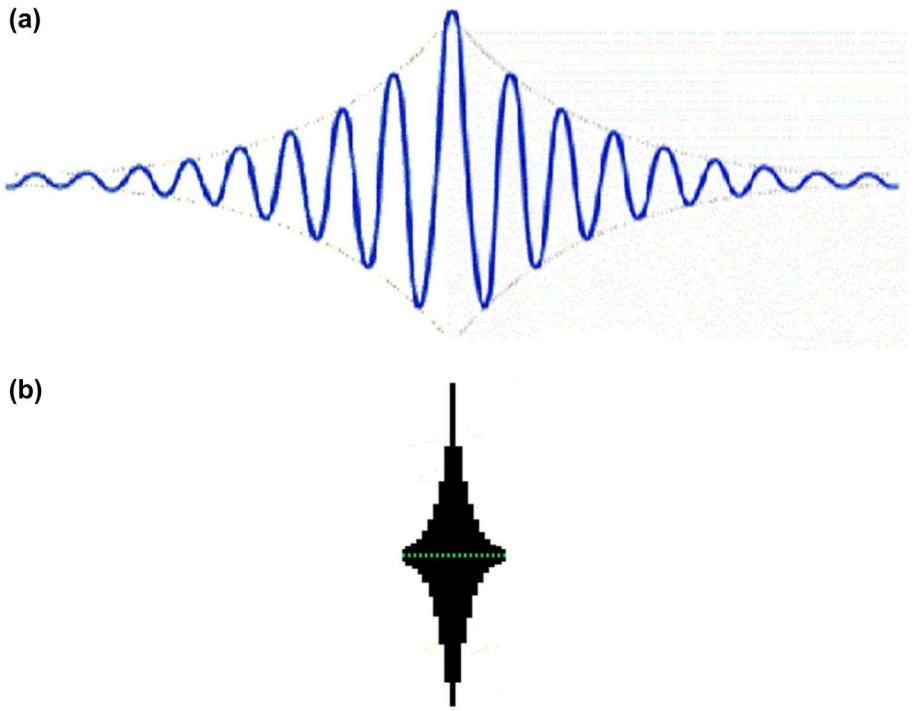

Figure 6. (a) A symmetrical environmental noise; and (b) the noise on the friction trace.

Figure 11 shows that, fibers of different fineness show different strain–stress behavior, which in turn results in different stick-slip behavior as shown in Figure 8. As is observed in Figure 11, strain of finer fibers is lower than that of coarser fibers. The reason for more stress of the finer fibers in comparison to coarser fibers can be explained in terms of constant draw ratio and variable spinning pump output. For a given constant draw ratio, any decrease or increase in pump output results in changes in fiber fineness. This is to say that when pump output is reduced, finer fibers are produced and more stress is exerted on them in comparison to the coarser fibers produced at higher pump output. The excess stress increases the extent of polymer chain re-arrangement and results in higher orientation degree of molecular chains. This exerts more stress on 6.9 denier fibers in comparison to 22.9

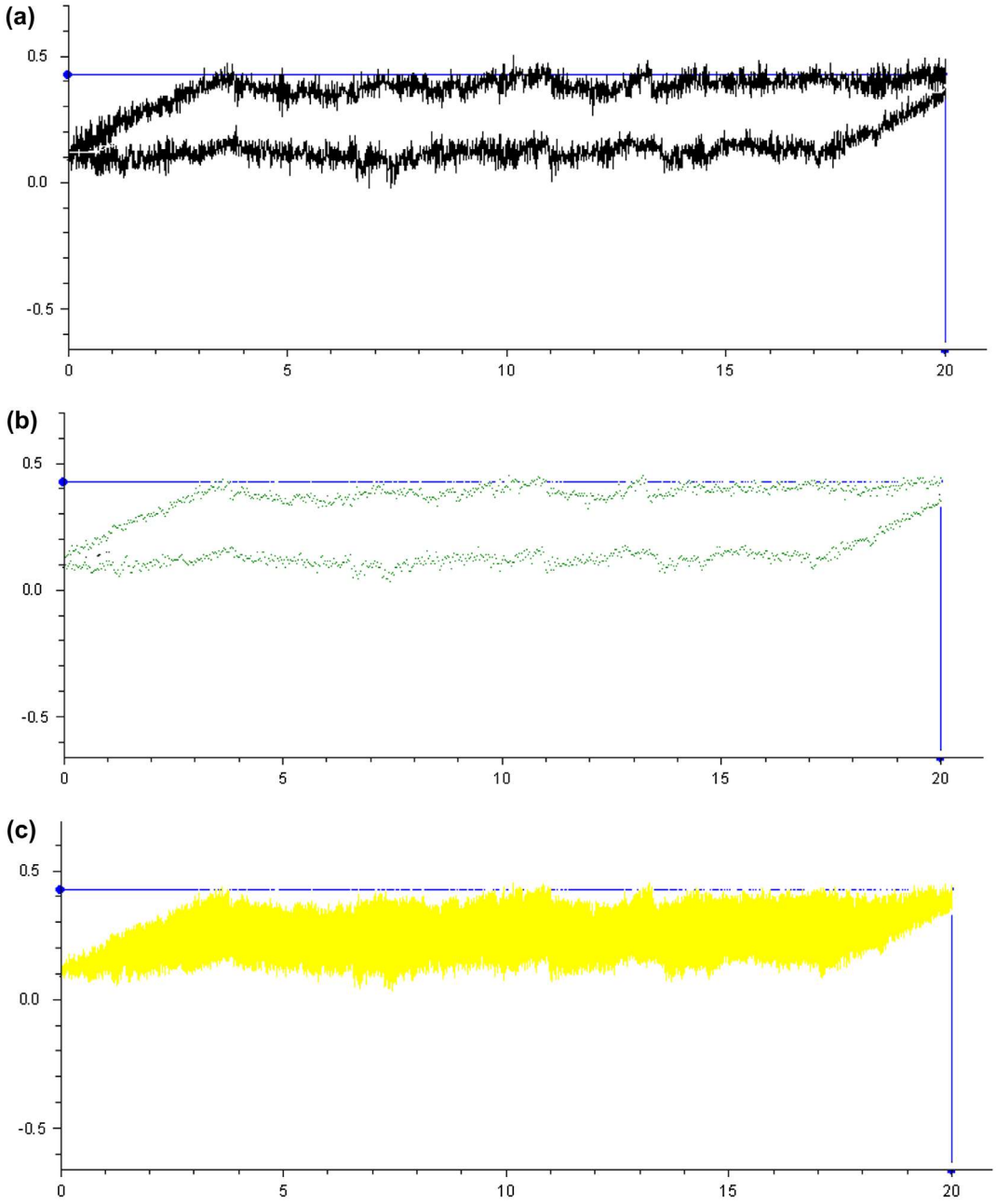

Figure 7. Delphi program operational steps (a) raw friction trace; (b) elimination of noises; and (c) calculation of work of friction.

Table 6. Variation of frictional force with fiber fineness.

Frictional force (cN)	Fiber fineness (den)	Fiber diameter (μm)
16.38	6.9	32.8
13.98	12.6	44.6
14.06	18.4	53.5
16.27	22.9	59.6

Table 7. Levene's test of homogeneity of variances.

Levene statistic	df1	df2	Sig.
0.432	3	116	0.731

denier fibers (Zarrebini, Mahmoudi, El-Bakary, El-Dessouky, & Lawrence, 2010). This is justification of the fact that friction traces for finer fibers are smoother and display much less fluctuation as compared with those of coarser fibers.

(3) During sliding of two fibers against each other, a significant amount of work dissipates as heat, although often it is very small as the area of contact is minute. However, since the dissipated heat is localized, the temperature rise at contact point can be quite substantial and may reach to several hundred degrees. In case of poor conductors like polymers, high localized temperatures may be reached even more readily (Gupta, 2008). Heat profile in the contact area of viscoelastic bodies depends on the radius of the contact point (Zeng, 2013). In the other words, fiber diameter affects geometry of the contact point and hence heat profile

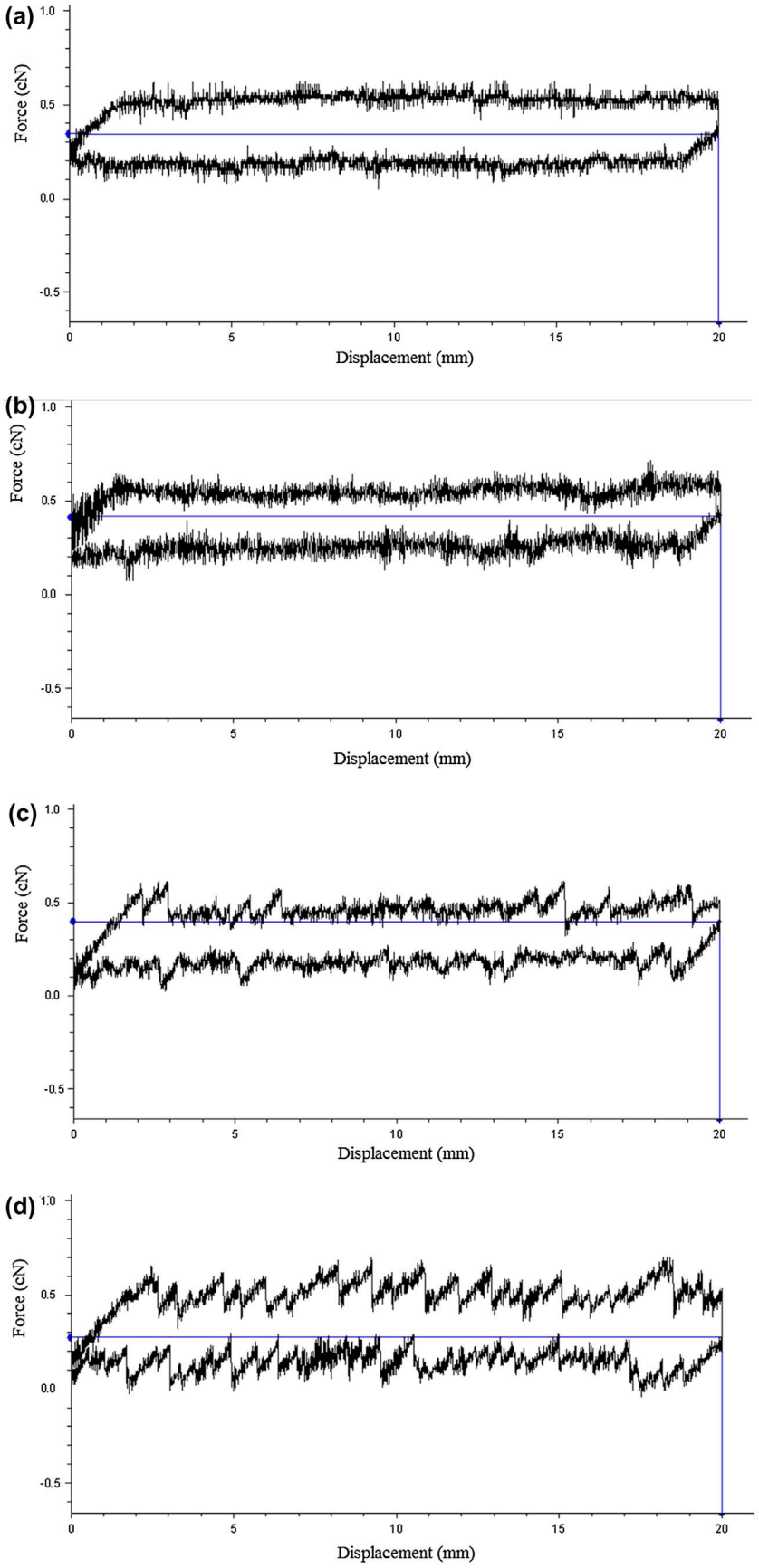

Figure 8. Stick-slip trace for fibers of (a) 6.9 denier; (b) 12.6 denier; (c) 18.4 denier; and (d) 22.9 denier.

Table 8. Descriptive analysis of mean values of frictional force.

	N	Mean	Std. deviation	Std. error	95% confidence interval for mean		Minimum	Maximum
					Lower bound	Upper bound		
1	30	16.3773	4.54303	0.82944	14.6809	18.0737	12.17	33.19
2	30	13.9831	3.12263	0.57011	12.8171	15.1491	8.54	22.38
3	30	14.0642	2.95031	0.53865	12.9626	15.1659	9.47	21.44
4	30	16.2704	3.78138	0.69038	14.8584	17.6824	10.00	27.18
Total	120	15.1737	3.78785	0.34578	14.4891	15.8584	8.54	33.19

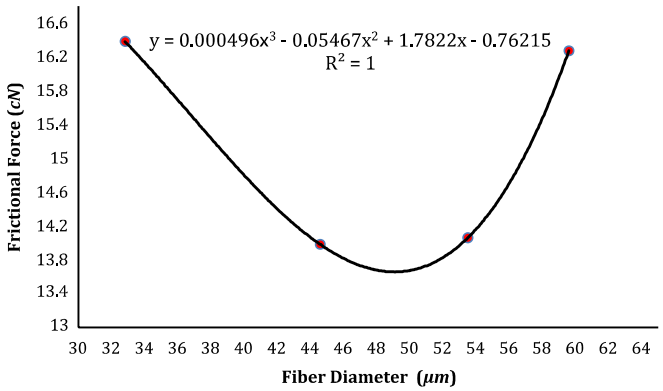

Figure 9. Frictional force versus fiber diameter.

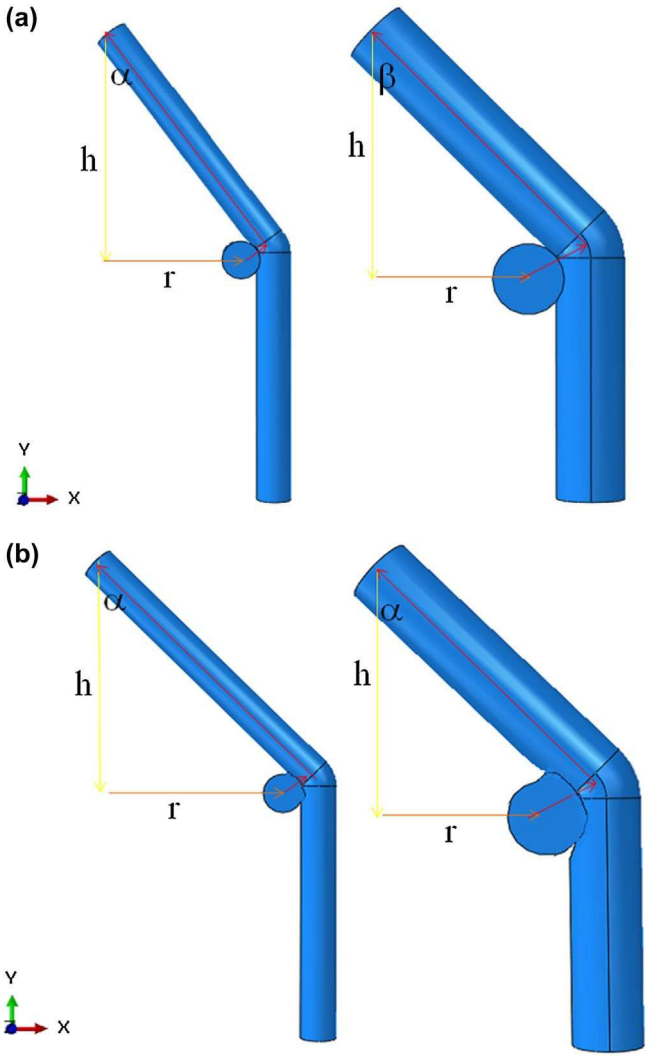

Figure 10. Contact area for (a) rigid materials; and (b) soft materials.

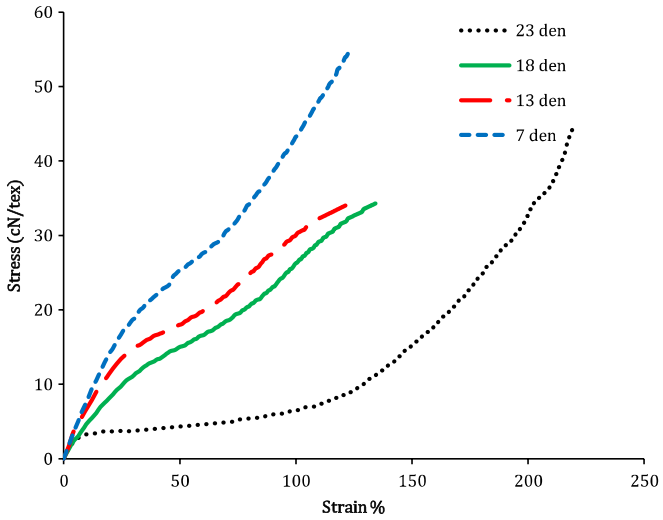

Figure 11. True stress–strain curve for fibers of different fineness.

at the contact point of two fibers cannot be similar. Hence, fibers with different diameters do not exhibit similar behavior during hanging fiber friction test.

5. Conclusion

In this work, the effect of fiber fineness on frictional behavior of polypropylene fibers was investigated. To this end, a high-precision setup based on hanging fiber method was developed. Additionally, a geometrical model capable of evaluating the frictional force between two in-contact identical fibers was proposed. A mathematical third-degree polynomial equation was proposed for calculating the frictional force between fibers. Using this equation, it was found that frictional force decreases with increasing fiber diameter up to a fiber diameter of 49.1 μm, beyond which it increases. The results vividly showed that, changes in fibers fineness leads to variation in stick-slip trace, which in turn affects the frictional force. It was found that factors such as geometry of contact area, fiber strain, and profile of the generated heat at contact area affect variation of fiber-frictional behavior with fiber diameter. The results of this study effectively is of use in various textile industries where the friction between fibers is of great importance including, but not limited to production of tops, drawing and spinning of short fibers into yarn, and non-woven industries.

Disclosure statement

No potential conflict of interest was reported by the authors.

Funding

This research received no specific grant from any funding agency in the public, commercial, or not-for-profit sectors.

ORCID

Mohammad Zarrebini http://orcid.org/0000-0002-0313-6998
Parham Soltani http://orcid.org/0000-0002-2153-3020

References

Abdellahi, B., Naghashzargar, E., & Semnani, D. (2016). Meso modeling of silk wire rope scaffolds in tissue engineering. *Journal of Industrial Textiles*, First Published May 12, 2016. doi: 10.1177/1528083716648762

Ajayi, J. O. (1992). Fabric smoothness, friction, and handle. *Textile Research Journal, 62*, 52–59.

Attaway, S. W. (1999). *The mechanics of friction in rope rescue*. Paper presented at the International Technical Rescue Symposium, Fort Collins, CO.

Bandyopadhyay, S. B. (1951). Frictional properties of jute and some other long vegetable fibers. *Textile Research Journal, 21*, 659–670.

Basu, S. C., Hamza, A. A., & Sikorski, J. (1978). The friction of cotton fibers. *Journal of the Textile Institute, 69*, 68–75.

Bhushan, B. (2013). *Introduction to tribology*. New York, NY: Wiley.

Briscoe, B. J. (1996). *Interfacial friction of solids*. Paper presented at the Solid-Solid Interactions: Proceedings of the First Royal Society-Unilever Indo-UK Forum in Materials Science and Engineering, London, UK.

Briscoe, B. J., & Kremnitzer, S. L. (1979). A study of the friction and adhesion of polyethylene-terephthalate monofilaments. *Journal of Physics D: Applied Physics, 12*(4), 505.

Briscoe, B. J., & Tabor, D. (1978). Friction and wear of polymers: The role of mechanical properties. *Polymer International, 10*, 74–78.

Campos, R., Bechtold, T., & Rohrer, C. (2003). Fiber friction in yarn – A fundamental property of fibers. *Textile Research Journal, 73*, 721–726.

Cho, D., Bhushan, B., & Dyess, J. (2016). Mechanisms of static and kinetic friction of polypropylene, polyethylene terephthalate, and high-density polyethylene pairs during sliding. *Tribology International, 94*, 165–175.

Cornelissen, B., de Rooij, M. B., Rietman, B., & Akkerman, R. (2014). Frictional behavior of carbon fiber tows: A contact mechanics model of tow–tow friction. *Textile Research Journal, 84*, 1476–1488.

Dintwa, E., Tijskens, E., & Ramon, H. (2008). On the accuracy of the Hertz model to describe the normal contact of soft elastic spheres. *Granular Matter, 10*, 209–221.

Gao, X., Wang, L., & Hao, X. (2015). An improved Capstan equation including power-law friction and bending rigidity for high performance yarn. *Mechanism and Machine Theory, 90*, 84–94.

Gralén, N., & Olofsson, B. (1947). Measurement of friction between single fibers. *Textile Research Journal, 17*, 488–496.

Gupta, B. S. (2008). *Friction in textile materials*. Cambridge, UK: Elsevier.

Gustafsson, E. (2013). *Investigation of friction between plastic parts*. Gothenburg: Chalmers University of Technology.

Guthrie, J. C., & Oliver, P. H. (1952). Inter-fiber friction of viscose rayon. *Journal of the Textile Institute Transactions, 43*, T579–T594.

Howell, H. G. (1951). Inter-fibre friction. *Journal of the Textile Institute Transactions, 42*, T521–T533.

Howell, H. G. (1953). The general case of friction of a string round a cylinder. *Journal of the Textile Institute Transactions, 44*, T359–T362.

Howell, H. G., & Mazur, J. (1953). Amontons' law and fiber friction. *Journal of the Textile Institute Transactions, 44*, T59–T69.

Kato, N., & Hirasawa, T. (1996). Effects of strain rate and strength nonuniformity on the slip nucleation process: A numerical experiment. *Tectonophysics, 265*, 299–311.

King, G. (1950). Some physical properties of wool and nylon fibers. *Journal of the Textile Institute Transactions, 41*, T135–T144.

Lincoln, B. (1954). The frictional properties of the wool fiber. *Journal of the Textile Institute Transactions, 45*, T92–T107.

Makinson, K. R. (1952). Some comments on the paper by Dr. N. Gralen. *Proceedings of the Royal Society of London, 212*, 495–496.

Marcicano, J. P. P., Tu, C. C., & Rylander, H. G. (2004). Measurement of the transverse yarn-on-solid coefficient of friction. *Journal of the Textile Institute, 95*, 349–357.

Martin, A. J. P., & Mittelmann, R. (1946). Some measurements of the friction of wool and mohair. *Journal of the Textile Institute Transactions, 37*, T269–T280.

Nair, A. U., Sheela, R., Vivekanandan, M. V., Patwardhan, B. A., & Nachane, R. P. (2013). Studies on friction in cotton textiles Part I: A study on the relationship between physical properties and frictional characteristics of cotton fibres and yarns. *Indian Journal of Fiber and Textile Research, 38*, 244–250.

Oxenham, W., & Hassanin, H. (1995). *A novel technique for assessing the frictional characteristics of cotton*. Paper presented at the Beltwide Cotton Conferences (USA), Memphis, TN.

Popov, V. L., & Heß, M. (2015). *Method of dimensionality reduction in contact mechanics and friction*. Heidelberg: Springer.

Rajanala, R. (2007). *Frictional study of polymeric textiles*. Lubbock, TX: Texas Tech University.

Ramkumar, S. S. (1998). *A study of the handle characteristics of 1×1 rib cotton weft knitted fabrics*. Leeds: University of Leeds.

Rubin, A., Favier, D., Danieau, P., Giraudel, M., Chambard, J. P., & Gauthier, C. (2016). Direct observation of contact on non transparent viscoelastic polymers surfaces: A new way to study creep and recovery. *Progress in Organic Coatings, 99*, 134–139.

Rusu, M., Daniela, I., Benchea, M., Carlescu, V., & Olaru, D. (2016). *Friction of the polymers-experimental results and analytical model*. Paper presented at the Applied Mechanics and Materials, *823*, 473–478.

Rusu, M., Ionita, D., Cârlescu, V., Prisacaru, G., & Olaru, D. (2015). Characterization of some types of polymers by friction behaviour. *Romanian Review Precision Mechanics, Optics & Mechatronics, 48*, 110.

Sinoimeri, A. (2009). Friction in textile fibers and its role in fiber processing. *Wear, 267*, 1619–1624. doi:10.1016/j.wear.2009.06.010

Soltani, P., & Johari, M. (2012). A study on siro-, solo-, compact-, and conventional ring-spun yarns. Part II: Yarn strength with relation to physical and structural properties of yarns. *Journal of the Textile Institute, 103*, 921–930.

Soltani, P., & Johari, M. S. (2012). Effect of strand spacing and twist multiplier on structural and mechanical properties of Siro-spun yarns. *Fibers and Polymers, 13*, 110–117.

Soltani, P., Johari, M. S., & Zarrebini, M. (2015). Tomography-based determination of transverse permeability in fibrous porous media. *Journal of Industrial Textiles, 44*, 738–756.

Soltani, P., Zarrebini, M., Laghaei, R., & Hassanpour, A. (2017). Prediction of permeability of realistic and virtual layered nonwovens using combined application of X-ray μCT and computer simulation. *Chemical Engineering Research and Design. 124*, 299–312 doi:10.1016/j.cherd.2017.06.035

Wang, Y., Miao, Y., Huang, L., Swenson, D., Yen, C. F., Yu, J., & Zheng, J. Q. (2016). Effect of the inter-fiber friction on fiber damage propagation and ballistic limit of 2-D woven fabrics under a fully confined boundary condition. *International Journal of Impact Engineering, 97*, 66–78. doi:10.1016/j.ijimpeng.2016.06.007

Zarrebini, M., Mahmoudi, M. R., El-Bakary, M. A., El-Dessouky, H. M., & Lawrence, C. A. (2010). The influence of fiber fineness on physical characteristics of staple polypropylene fibers spun at different pumping speeds. *Journal of Applied Polymer Science, 115*, 2892–2897. doi:10.1002/app.31333

Zeng, H. (2013). *Polymer adhesion, friction, and lubrication*. New York, NY: Wiley.

Zhang, J., Butz, A., & Li, Q. (2016). Simulation of frictional energy dissipation in a fiber contact subjected to normal and tangential oscillation. *Physical Mesomechanics, 19*, 173–177.